RESEARCH ARTICLE

WILEY | Journal of **Cellular Biochemistry**

Inhibition of the chimeric DnaJ-PKAc enzyme by endogenous inhibitor proteins

April M. Averill[1] | Hibba tul Rehman[2,3] | Joseph W. Charles[4] | Timothy A. Dinh[5,6] | Karamatullah Danyal[7] | Claire F. Verschraegen[8] | Gary S. Stein[3,9] | Wolfgang R. Dostmann[4] | Jon E. Ramsey[3,9]

[1]Department of Microbiology and Molecular Genetics, Larner College of Medicine, University of Vermont, Burlington, Vermont

[2]Division of Hematology and Oncology, Department of Medicine, Larner College of Medicine, University of Vermont, Burlington, Vermont

[3]University of Vermont Cancer Center, Burlington, Vermont

[4]Department of Pharmacology, Larner College of Medicine, University of Vermont, Burlington, Vermont

[5]Department of Biomedical Sciences, College of Veterinary Medicine, Cornell University, Ithaca, New York

[6]Curriculum in Genetics and Molecular Biology, University of North Carolina at Chapel Hill, Chapel Hill, North Carolina

[7]Department of Pathology, Larner College of Medicine, University of Vermont, Burlington, Vermont

[8]Division of Medical Oncology, The Ohio State Comprehensive Cancer Center, Columbus, Ohio

[9]Department of Biochemistry,, Larner College of Medicine, University of Vermont, Burlington, Vermont

Correspondence
Jon E. Ramsey, Department of Biochemistry, University of Vermont, Burlington, VT 05405.
Email jeramsey@uvm.edu

Abstract

The chimeric DnaJ-PKAc enzyme resulting from an approximately 400-kb deletion of chromosome 19 is a primary contributor to the oncogenic transformation that occurs in fibrolamellar hepatocellular carcinoma, also called fibrolamellar carcinoma (FLC). This oncogenic deletion juxtaposes exon 1 of the DNAJB1 heat shock protein gene with exon 2 of the PRKACA gene encoding the protein kinase A catalytic subunit, resulting in DnaJ-PKAc fusion under the transcriptional control of the DNAJB1 promoter. The expression of DnaJ-PKAc is approximately 10 times that of wild-type (wt) PKAc catalytic subunits, causing elevated and dysregulated kinase activity that contributes to oncogenic transformation. In normal cells, PKAc activity is regulated by a group of endogenous proteins, termed protein kinase inhibitors (PKI) that competitively inhibit PKAc and assist with the nuclear export of the enzyme. Currently, it is scarcely known whether interactions with PKI are perturbed in DnaJ-PKAc. In this report, we survey existing data sets to assess the expression levels of the various PKI isoforms that exist in humans to identify those that are candidates to encounter DnaJ-PKAc in both normal liver and FLC tumors. We then compare inhibition profiles of wtPKAc and DnaJ-PKAc against PKI and demonstrate that extensive structural homology in the active site clefts of the two enzymes confers similar kinase activities and inhibition by full-length PKI and PKI-derived peptides.

KEYWORDS

fibrolamellar hepatocellular carcinoma, inhibition, kinase activity, liver, protein kinase A

1 | INTRODUCTION

Fibrolamellar hepatocellular carcinoma, also called fibrolamellar carcinoma (FLC), is a rare and aggressive form of liver cancer for which the only effective treatment is surgical excision. It encompasses 1% to 5% of liver cancers and incidence rates are increasing. Treatment limitations, especially for metastatic FLC, have resulted in poor overall survival with less than a 3% 5-year survival rate for patients afflicted with metastatic disease (www.cancer.org/acs). FLC predominantly affects young adults with an average age of diagnosis approximately 19 years.[1,2] FLC is characterized by a chromosomal translocation that deletes approximately 400 kb of chromosome 19, resulting in the fusion of exon 1 of the DNAJB1 heat shock protein gene with exon 2 of the PRKACA gene encoding the protein kinase A catalytic subunit. This deletion gives rise to a unique chimeric transcript that is found exclusively and universally in FLC tumors and appears to be necessary and sufficient for the development of the disease.[3,4] No other genetic lesions consistently associate with the disease.[1,2] This translocation has not been reported in any other cancers.

The DNAJB1-PRKACA transcript encodes a functional chimeric kinase, termed DnaJ-PKAc, in which the 15 amino-terminal amino acids of wtPKAc are replaced with approximately 70 amino acids from the amino terminus of DnaJ. The exclusivity of DnaJ-PKAc in FLC has provided the basis for investigation into its roles in disease progression and whether it represents an effective target for treatment. The chimeric protein has comparable kinase activity to that of wild-type PRKACA (wtPKAc) toward peptide substrates in vitro.[5] The chromosomal translocation puts the expression of the chimeric gene under control of the endogenous DNAJB1 promoter, which provides constitutive expression at a level approximately 10 times that of wtPRKACA.[4] This robust expression elevates chimeric protein expression to exceed the amounts of regulatory domain proteins necessary to limit kinase activity. It is hypothesized that transformation occurs due to a compromised control of kinase activity, leading to increased rate of proliferation, cytoplasmic-nuclear ratios, nucleolar size, and protein secretion that drives the fibrolamellar structure formation within the unique tumor stroma that is the hallmark of the disease.[6,7] For these reasons, DnaJ-PKAc is widely perceived to be a good candidate target for pharmacological intervention.

To date, efforts to develop small molecule competitive inhibitors of DnaJ-PKAc have been unsuccessful. Seminal findings by Cheung et al[5] established remarkable structural similarities between DnaJ-PKAc and wtPKAc, especially in the active site domain. These observations may be the basis for difficulties in identifying selective competitive inhibitors that target DnaJ-PKAc, while avoiding wtPKAc. The essential function of PKAc—especially in the liver, where it regulates glycogen catabolism—makes selectivity a crucial characteristic of targeted inhibitors, should one be found. Furthermore, Cheung et al also showed that DnaJ-PKAc retains several additional activities of wtPKAc that are of interest, physiologically. Specifically, DnaJ-PKAc shows similar parameters of binding to regulatory subunits RIα and RIIβ and maintains binding to the canonical A-kinase anchoring protein, AKIP1a, despite that this interaction is mediated by the N-terminal domain of wtPKAc.[8] It has been speculated that small perturbations in the ATP binding site of DnaJ-PKAc,[5] in addition to the unique functions contributed by the DnaJ portion of DnaJ-PKAc, may represent targetable attributes in FLC. However, advancements toward these ends have not yet been reported.

In the physiological context, the PKAc activity is confined by a multitude of mechanisms. In addition to cyclic adenosine monophosphate (cAMP) attenuation, regulatory subunit binding, and anchoring at specific cellular locations by A-kinase anchoring proteins, direct competitive inhibition of PKAc is accomplished by four distinct endogenous peptide inhibitors. In humans, this repertoire is encoded by three genes that produce protein kinase inhibitor-α (PKIα), two splice variants of PKIβ, and PKIγ. The role of these peptides, that range in size from 76 to 85 amino acids, is to attenuate PKAc activity after cAMP-mediated activation and export of PKAc from the nucleus.[9] Several studies have demonstrated that activity of these peptides is critical for attenuating PKA-mediated early response gene expression and shuttling PKAc from the nucleus, allowing cellular specification and proper tissue development.[10,11] Differential tissue expression of these peptides further supports their roles in modulating PKA signaling, predominantly in the nucleus, and is critical in the fidelity of tissue development and physiological control.[12,13] It is not currently known whether endogenous PKI-mediated inhibition of PKA signaling is altered in the context of DnaJ-PKAc-mediated pathogenesis of FLC. In this study, we compared activity and inhibition of DnaJ-PKAc and wtPKAc by short peptide inhibitors derived from PKI and by full-length PKI. We examined PKI gene expression in FLC tumor cells in addition to liver cell lineages. We demonstrate that the in vitro inhibition profile of DnaJ-PKAc by PKIβ is indistinguishable from that of wtPKAc.

2 | MATERIALS AND METHODS

2.1 | Plasmids, protein expression, and purification

A complementary DNA (cDNA) encoding DnaJ-PKAc in pLATE11 was gifted to us by Dr Wayne Hendrickson (Columbia University). A cDNA insert for wtPKAc was supplied in plasmid pRSET-B (Invitrogen, Waltham, MA) as a kind gift from Dr Friedrich W. Herberg (Kassel University). wtPKAc was subsequently cloned into pLATE31-LIC (Thermo Fisher Scientific) using appropriate oligonucleotide polymerase chain reaction primers, according to the manufacturuer's instructions. Both expression constructs were individually transformed into Rosetta2(DE3)pLysS competent cells (Novagen, Madison, WI) and plated onto an LB-agar plate supplemented with 100 μg/mL ampicillin and 34 μg/mL chloramphenicol. Protein expression was performed using a variation of the autoinduction method.[14] From a freshly transformed plate, approximately 20 colonies were used to inoculate 1 L of terrific broth (Affymetrix, Inc, Cleveland, Ohio) supplemented with 50 μg/mL of ampicillin and 1× 5052 autoinduction solution (0.5% glycerol, 0.05% glucose, and 0.2% α-lactose). Cultures were grown in a 2.8-L Fernbach flask (Fisher Scientific, Hampton, NH) and were shaken at 20°C for approximately 60 hours; then the cells were harvested and stored at −80°C.

To purify wtPKAc and DnaJ-PKAc, frozen cell pellets were thawed on ice and resuspended in lysis buffer (20 mM Tris, pH 7.0, 500 mM NaCl, 10 mM imidazole, 5 mM β-mercaptoethanol, 10% glycerol, and 1× Roche Complete EDTA-Free Protease Inhibitor). Cells were lysed by sonication and cleared by centrifugation. A HisTrap HP column (GE Healthcare, Piscataway, NJ) was equilibrated in five column volumes of binding buffer (20 mM Tris, pH 7.0, 500 mM NaCl, 10 mM imidazole, 5 mM β-mercaptoethanol, and 10% glycerol), and the cleared lysate was loaded onto the column using an ÄKTA Purifier (GE Healthcare). The column was washed with five column volumes of binding buffer followed by a linear gradient from 10 to 500 mM imidazole in binding buffer (20 mM Tris, pH 7.0, 500 mM NaCl, 5 mM β-mercaptoethanol, and 10% glycerol). Fractionated protein was pooled after sodium dodecyl sulfate polyacrylamide gel electrophoresis (SDS-PAGE) analysis. Pooled fractions were dialyzed overnight in 20 mM Tris, pH 7.0, 300 mM NaCl, 5 mM β-mercaptoethanol, and 10% glycerol. After removing from dialysis, the protein solution was further diluted to a final salt concentration of 150 mM NaCl and loaded onto an SP-FF column (GE Healthcare) equilibrated in fast flow sepharose (FFS) buffer (20 mM Tris, pH 7.5, 150 mM NaCl, 5 mM β-mercaptoethanol, and 10% glycerol). The column was washed with five column volumes of FFS buffer, and protein was eluted with 20 column volumes linear salt gradient from 150 mM to 1 M NaCl in FFS buffer. On the basis of the results of SDS-PAGE analysis, fractions containing pure protein were pooled, concentrated, and flash frozen.

2.2 | Structure and sequence analyses

Atomic coordinate files for wtPKAc (2GFC) and chimeric DnaJ-PKAc (4WB7), both in complex with ATP analogs and PKI inhibitor peptides, were retrieved from the Research Collaboratory for Structural Bioinformatics Protein Database (www.rcsb.org). Structural alignments, intra- and intermolecular distance measurements, Cα root-mean-square deviation (RMSD) calculations, and image renderings were performed using the PyMol software (Schrödinger, Inc, Cambridge, MA). For PKI sequence analysis, amino acid sequences for human PKIα (accession CAG33333), PKIβ1 (NP_861460), PKIβ2 (accession NP_001257324), and PKIγ (accession NP_001268374) were retrieved from the Nation Center for Biotechnology Information Database (www.ncbi.nlm.nih.gov) and aligned using ClustalOmega (www.ebi.ac.uk).

2.3 | Enzyme activity assay

Kinase activity of recombinant wtPKAc and DnaJ-PKAc toward the synthetic substrate peptide (W15, TQAKRKK-SLAMA) was measured by a γ^{32}P-ATP incorporation assay, as described with some modifications.[15] Briefly, reactions were initiated when 0.1 mM γ^{32}P-ATP (200-300 counts per minute [cpm]/pmol; Perkin Elmer, Waltham, MA) was added to vials preincubated with 50 mM 2-(N-morpholino)ethanesulfonic acid (MES), pH 6.9, 1 mM magnesium acetate, 10 mM sodium chloride, 10 mM dithiothreitol, 1 mg/mL bovine serum albumin, 0 to 62 μM W15 substrate (serially diluted), and 1 nM purified enzyme in 100 μL reaction volume at 30°C. Before the initiation of the reaction, all components excluding γ^{32}P-ATP were allowed to preincubate for 5 minutes. Each reaction was run for 90 seconds at 30°C and terminated by blotting 50 μL of reaction solution on 25 mm phosphocellulose circles (Whatman P81 filter paper; GE Life Sciences, Piscataway, NJ). Filters were washed three times in 0.8% phosphoric acid and measured by liquid scintillation counting. Data were analyzed using Excel (RRID: SCR_016137; Microsoft, Redmond, WA) and Prism 6 (RRID: SCR_002798; GraphPad, San Diego, CA), by fitting to the conventional Michaelis-Menten enzyme kinetic model.

2.4 | Enzyme inhibition assay

Protein Kinase A Inhibitor Fragment 6-22 amide was purchased from Sigma (catalog number P6062; Sigma, St. Louis, MO). Recombinant PKIβ was obtained from Novus Biologicals, Centennial, CO (catalog number NBP1-51058). Inhibition profiles of wtPKAc and DnaJ-PKAc were obtained by performing activity assays, as described above with minor modifications. Purified enzymes (2 nM) were preincubated with 50 mM MES, pH 6.9, 1 mM magnesium acetate, 10 mM sodium chloride, 10 mM dithiothreitol, 1 mg/mL bovine serum albumin, and various concentrations of inhibitors (serially diluted) at 30°C for 5 minutes. Reactions were initiated by the addition of 0.1 mM γ^{32}P-ATP (200-300 cpm/pmol) and 10 μM W15 substrate in a final volume of 100 μL. Reactions were allowed to proceed for 90 seconds at 30°C and terminated by blotting 50 μL of reaction solution on 25-mm diameter phosphocellulose filter paper (Whatman P81 filter paper; GE Life Sciences, Piscataway, NJ). Filters were washed and counted as above. Data were analyzed using Excel and Prism 6 by fitting to a four-parameter inhibition model to obtain the best fit IC_{50} values.

3 | RESULTS

3.1 | PKAc and DnaJ-PKAc display similar kinase activity and peptide-based inhibition profiles

On the basis of previously reported observations and a re-examination of the crystal structures reported for wtPKAc and DnaJ-PKAc, we predicted that kinase activity toward small peptide substrates (5-15 amino acids) would be similar. Figure 1A shows an overlay of structure models of DnaJ-PKAc and wtPKAc. The RMSD of Cα atoms was computed to be 0.333 Å for the 311 shared amino acids, exemplifying the degree of structural conservation. Visual inspection of the active site (Figure 1B) reinforces active site congruity, as conservation is largely extended to both enzyme constituents and peptide inhibitor (PKIα 5-22) geometry. Although slight deviations are observed in the C-terminus of PKIα 5 to 22 and neighboring enzyme active site residues, the analysis suggests that wtPKAc and DnaJ-PKAc display similar phosphoryl transferase kinetics and inhibitor affinity. To test these predictions, wtPKAc and chimeric DnaJ-PKAc were expressed in *Escherichia coli*
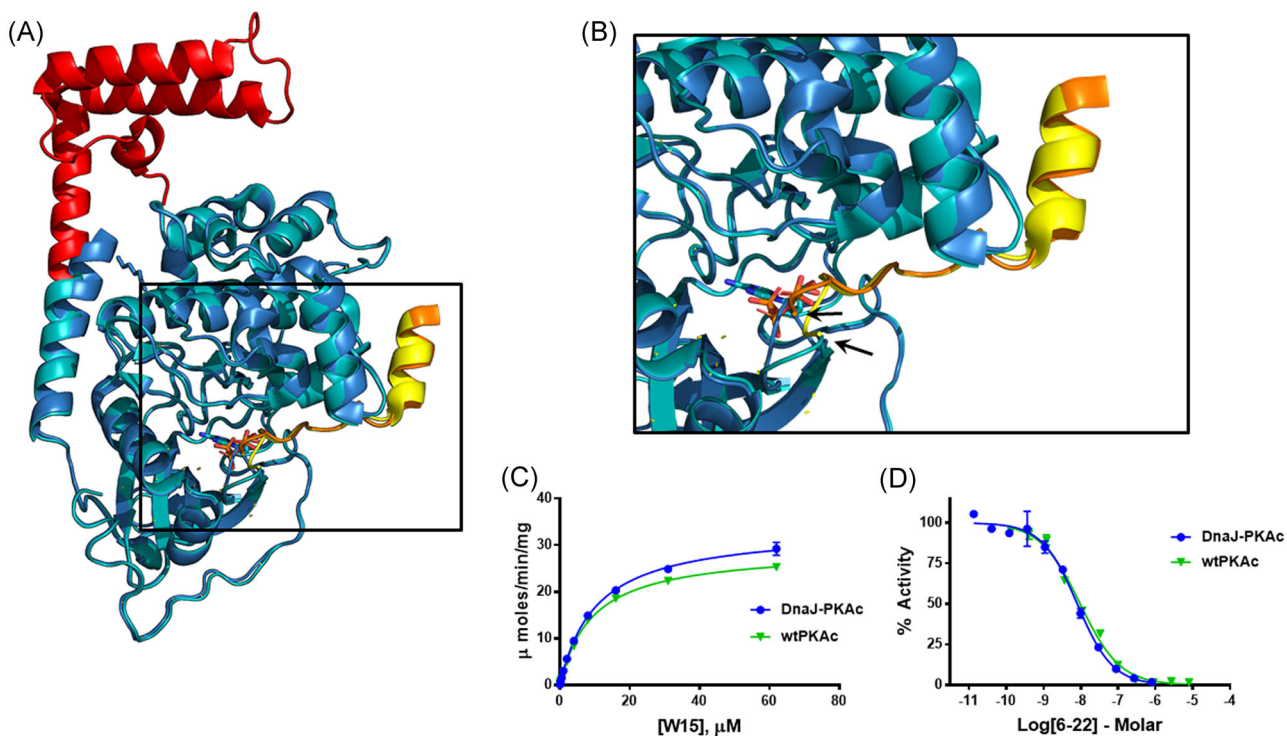

FIGURE 1 Structural similarities between wtPKAc and DnaJ-PKAc underlie similarities in activity and inhibition by PKI peptide. A, Crystal structure models of wtPKAc (blue) and DnaJ-PKAc (red/cyan) were aligned in PyMol. The DnaJ portion of DnaJ-PKAc is highlighted in red. The active site cleft is indicated by the box. B, The structures of PKIα 5 to 22 in complex with wtPKI (yellow) and DnaJ-PKAc (orange) are also overlayed. Structural deviations in both PKIα 5 to 22 and enzyme backbones are highlighted with arrows. C, Michaelis-Menten kinetic profiles of wtPKAc and DnaJ-PKAc for peptide substrate W15. Symbols represent mean values (±standard error) of replicate experiments. Lines represent the best fit to the Michaelis-Menten equation. D, Comparison of wtPKAc and DnaJ-PKAc activity inhibited by 6-22. Symbols represent mean values (±standard error) of replicate experiments. Lines represent the best fit to a four-parameter inhibition model. PKI, protein kinase inhibitor; wt, wild type

and purified to homogeneity using a combination of immobilized metal affinity and cation exchange chromatography. Kinase activity was measured for both enzymes using a conventional kinase activity assay[15] that incorporates a model peptide substrate designated W15.[16] Both enzymes displayed near-identical Michaelis-Menten kinetic parameters toward W15 (Figure 1C; Table 1), with activities similar to those reported previously toward the Kemptide substrate.[5] These results not only confirmed our predictions that activities toward these and other small peptide substrates would be consistently similar between wtPKAc and DnaJ-PKAc due to the high degree of active site structural similarities observed between the wild-type and chimeric proteins. These results also showed that our enzyme preparations were highly active.

To test inhibitor affinity, we used PKIα 6-22 amide (referred to herein as 6-22) in W15 phosphorylation reactions catalyzed by equimolar amounts of either wtPKAc or DnaJ-PKAc. We observed that 6-22 potently inhibits both enzymes with near-equal IC_{50} values (Figure 1D; Table 1). These results support the concept that active site structural similarities that exist between the wild-type and chimeric proteins manifest as compare to binding affinities of inhibitor peptides.

3.2 | PKI gene expression in normal liver and FLC tumors

Despite a growing understanding of DnaJ-PKAc biochemistry, there is minimal knowledge whether inhibition by endogenous PKAc inhibitors (PKI) is perturbed in the fusion protein, predominantly in liver cell lineages and FLC tumors. Figure 2A shows a sequence alignment of the four human PKI isoforms. A high degree of conservation exists amongst the four isoforms, particularly in the regions corresponding to the "core binding domain" from which most PKAc inhibitory peptides are derived, and in the nuclear export signal (NES) region. To assess expression of PKI in normal liver tissues and FLC tumors, we surveyed publicly available data sets in the Genotype-Tissue Expression Project (GTEx), the Human Protein Atlas (HPA), the Gene Expression Omnibus, and The Cancer Genome Atlas (TCGA). These queries yielded several data sets that allowed for assessment of PKI messenger RNA (mRNA) levels in normal liver tissues, two that permitted comparison of PKI transcript quantitation between normal liver and FLC tumor tissue (GSE63018[17] and TCGA[18]) and one that allowed comparison between the FLC cell line Tu2010 against four culture models of liver maturational stage cell types (GSE73114[19]). Hybridization and sequencing techniques did not permit differentiation of the PKIβ splice variant isoforms. Isoform expression profiling in normal liver

tissues (Figure 2B-D) shows that GPKIG is the PKI transcript that is consistently expressed at the highest levels in normal liver tissues/cell types. PKIA and PKIB transcripts are considerably lower in all data sets; however, some inconsistencies emerge in the ranking expression of these two isoforms. In the HPA, GTEx, and TCGA data sets (Figure 2B-D, respectively), PKIA is often at or below the threshold of detection, with PKIB slightly higher. However, in the GSE63018 data set, this ranking is reversed (Figure 2E). Curiously, in culture models of adult hepatocytes, biliary tree stem cells (BTSCs), hepatoblasts, hepatic stem cells, FLC tumors, and PKI expression exhibit a variation (Figure 2F). PKIG appears to, again, be highest in adult hepatocytes and FLC tumors (FLHCC). PKIB appears to be the predominant transcript in BTSCs and hepatic stem cells. PKIA transcript levels are near detection threshold limits in all cell types.

At the protein level, much less is known about PKI in human liver tissue. There is limited data available at this time from the HPA. These data indicate that PKIβ is highly expressed, PKIγ exhibits medium expression levels, and PKIα is very low. This is in slight contrast to transcriptional data, as described above, which suggests PKIG to be the predominant PKI, followed by PKIB, and PKIA.

3.3 | Inhibition of wtPKAc and DnaJ-PKAc by full-length PKI

As structural models and our experimental evidence indicate significant similarities between the active site cleft regions of wtPKAc and DnaJ-PKAc confer consistent catalytic activities and enzyme inhibition in the context of either low molecular weight peptide substrates or inhibitors, respectively. Structural differences between wtPKAc and DnaJ-PKAc exist outside the active site cleft,

TABLE 1 Kinetic and inhibition properties of wtPKAc and DnaJ-PKAc[a]

Parameter	wtPKAc	DnaJ-PKAc
V_{max}	29.15 μmoles/min (28.52 to 29.79)	33.68 μmoles/min (32.84 to 34.56)
K_m	9.26 μM (8.68 to 9.88)	10.3 μM (9.55 to 11.1)
IC_{50}		
6-22	9.65 nM (8.44 to 11.04)	8.05 nM (6.94 to 9.34)
PKIβ1	6.63 nM (5.24 to 8.27)	5.91 nM (3.36 to 9.52)

Abbreviations: IC, inhibitory concentration; PKI, protein kinase inhibitor; wt, wild type.

[a]Values represent global best fit values of data to Michaelis-Menten equation (V_{max}, K_m), or to four-parameter inhibition model (IC_{50}). 95% confidence intervals indicated in parentheses.
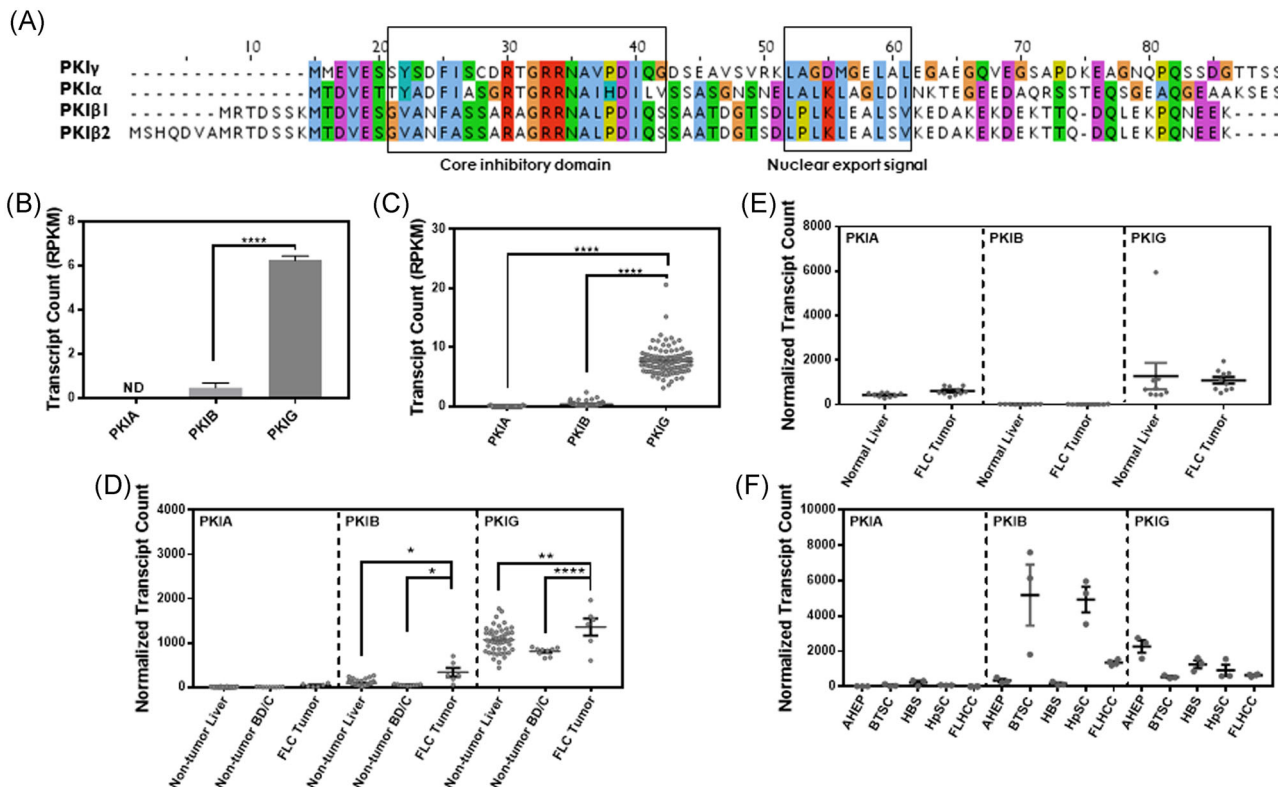
FIGURE 2 PKI isoform expression in human tissues and tissue culture models of liver maturation. (A) Primary amino acid sequence alignment of the four PKI isoforms expressed in humans. Conserved domains are highlighted. PKI isoform mRNA levels found in normal human liver as reported in the Human Protein Atlas (B) and in GTEx (C) databases. Comparative analysis of PKI expression in nontumor liver, nontumor biliary duct/cholangiocytes (BD/C) and FLC tumor, as reported in TCGA (D) and in GSE63018 (E). (F) PKI expression in cell culture models of adult hepatocytes (AHEP), biliary tree stem cells (BTSC), hepatic stem cells (HpSC), and FLC tumors (FLHCC). Unpaired t test (B) or ANOVA tests with multiple comparison corrections (C-F) were performed to determine the statistical significance of differences between mean values, where applicable. $*P < 0.05$, $**P < 0.005$, $****P < 0.0001$. ANOVA, analysis of variance; GTEx, Genotype-Tissue Expression Project; mRNA, messenger RNA; PKI, protein kinase inhibitor; TCGA, The Cancer Genome Atlas
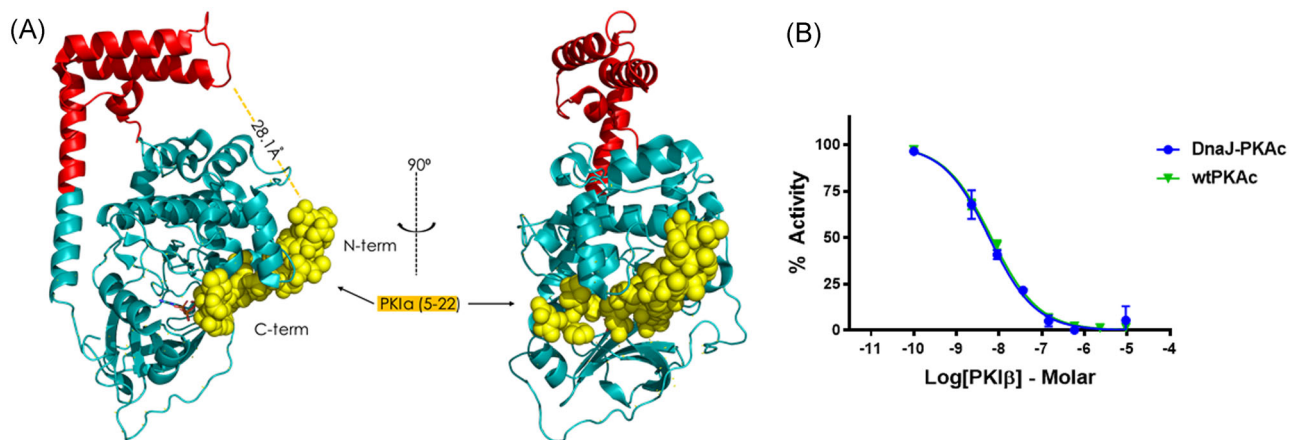

FIGURE 3 Inhibition of DnaJ-PKAc by PKIβ is indistinguishable from that of wtPKAc. A, Structural analysis of DnaJ-PKAc in complex with PKIα 5 to 22 shows proximity of unique DnaJ moiety and the N-terminus of the inhibitory peptide. The distance of the closest atomic coordinates from both constituents was measured to be 28.1 Å. B, Comparison of wtPKAc and DnaJ-PKAc activity inhibited by PKIβ. Symbols represent mean values (±standard error) of replicate experiments. Lines represent the best fit to a four-parameter inhibition model. PKI, protein kinase inhibitor; wt, wild type

particularly in the N-terminal region that corresponds to the juxtaposed DnaJ fragment of the chimeric protein (Figure 3A). To determine whether this bulky structural addition interferes with binding of larger inhibitors, we used a full-length PKIβ that we obtained from a commercial source (Novus Biologicals) in our inhibition assay. Recombinant full-length PKIβ (isoform 1), as it is supplied from the vendor (Novus Biologicals) is considerably larger than the 6-22 inhibitor peptide, as it contains the full 76 amino acid sequence plus an additional 20 amino acids at the N-terminus that correspond to a polyhistidine purification tag. We hypothesized that the addition of approximately 27 residues to the N-terminal side of the core inhibitor-binding region may disrupt interactions with the DnaJ portion of the chimeric enzyme, as it appears to be approximately 28 Å away in the crystal structure model (Figure 3A). However, full-length human PKIβ (isoform 1) showed equal inhibitory activity towards wtPKAc and DnaJ-PKAc (Figure 3B), suggesting that the additional amino acids that reside outside of the core inhibitory domain of PKIβ1 do not contribute to a discriminatory interaction. Currently, no structures of full-length PKI, either alone or in complex with PKAc, have been deposited to the Research Collaboratory for Structural Bioinformatics Protein Database (www.rcsb.org). Thus, it is difficult to predict the conformation of the additional residues in the context of the inhibited complex formed with either wtPKAc or DnaJ-PKAc.

4 | DISCUSSION

There is growing experimental and observational evidence that suggests the chimeric DnaJ-PKAc enzyme produced as a consequence of the partial deletion of chromosome 19 is a decisive factor resulting in FLC tumors.[20] Accordingly, DnaJ-PKAc is regarded as a viable candidate for pharmacological interventions FLC. Reports on inhibition of DnaJ-PKAc, both by endogenous inhibitory proteins (PKI) and small molecules are limited. The essential function of wtPKAc in the liver, as a regulator of glycogen metabolism and gene transcription, makes specificity an important consideration in inhibitor design and/or discovery. Inhibitor specificity is restricted by strong structural similarities in the active site clefts of wtPKAc and DnaJ-PKAc (Figure 1A).

DnaJ-PKAc inhibition by short peptides derived from endogenous PKI and by full-length PKI is similar. Furthermore, comparative analysis of existing crystallographic structures of wtPKAc and DnaJ-PKAc shows that phosphoryl transferase activities and competitive inhibition profiles with short peptides are indistinguishable between the two enzymes. Kinase activity of both enzymes using the W15 substrate is indistinguishable, consistent with previous reports using the Kemptide substrate.[5] Similarly, inhibition profiles of wtPKAc and DnaJ-PKAc by way of the 6-22 peptide derived from human PKIα are nearly identical.

We interrogated several publicly available data sets to identify which PKI paralog(s) can be expected to be present in human liver and FLC tumors. At the mRNA level, it is evident that PKIG is expressed at higher levels than either PKIA or PKIB in human tissues (Figure 2B-E). In tissue culture models of four liver maturational stage cell types and the FLC tumor line Tu2010, expression of the three primary PKI isoforms is more varied and complex. It is possible that isolation and/or culturing of these cell lines created a shift in PKI gene expression. Summarily, these results suggest that PKIB is the most predominant PKI mRNA expressed in both FLC tumors and in BTSCs, the proposed cells of origin for FLC tumors.[19]

We hypothesized that the additional structure contributed by the DnaJ portion of the chimeric enzyme provides sufficient bulk to interact, either productively or nonproductively, with the N-terminal region of full-length PKI molecules. This concept was based on the proximity of the N-terminus of the PKI (5-22) inhibitor peptide and the DnaJ domain observed in the crystal structure model of DnaJ-PKAc (Figure 3A). Counter-intuitively, we observed no difference in inhibition of wtPKAc vs DnaJ-PKAc by full-length PKIβ with an additional N-terminal purification tag (Figure 3B). Unfortunately, the configuration and orientation of the N-terminus of PKI relative to wtPKAc or DnaJ-PKAc in the context of an inhibited complex are not currently known. It is possible that purification tag substituents present in the recombinant PKIβ utilized here are obscuring the measured IC_{50} values. Although polyhistidine affinity tags typically do not adopt stable secondary structures,[21] their presence has been found to alter structure/dynamics,[22] activity/function,[23] and stability[24-27] of various proteins. It is possible that, in this case, the polyhistidine affinity is contributing disorder in the N-terminal region of PKIβ1 precluding interaction with the DnaJ domain of DnaJ-PKAc.

Within the context of its pathological role in FLC, our data suggest that DnaJ-PKAc kinase activity is not refractory to inhibition by PKIβ, one of the primary PKI isoforms present in both normal liver and FLC tumors. It is likely that DnaJ-PKAc levels, resulting from transcriptional dysregulation associated with the signature deletion within chromosome 19, overwhelms PKI levels, thus permitting heightened kinase activity that is observed in FLC.[7] It remains to be determined whether nuclear export properties are perturbed in the context of the DnaJ-PKAc/PKIβ complex, although previous reports

have found that nuclear localization of PKAc subunits in relation to total cellular PKAc subunits to actually be decreased in FLC compared with normal liver.[7] This aspect of FLC etiology, as well as inhibition of DnaJ-PKAc by PKIγ, will be the focus of future research efforts.

CONFLICT OF INTERESTS

The authors declare that there are no conflict of interests.

ORCID

Jon E. Ramsey http://orcid.org/0000-0001-6349-902X

REFERENCES

1. Eggert T, McGlynn KA, Duffy A, Manns MP, Greten TF, Altekruse SF. Fibrolamellar hepatocellular carcinoma in the USA, 2000-2010: a detailed report on frequency, treatment, and outcome based on the surveillance, epidemiology, and end results database. *United Eur Gastroenterol J*. 2013;1(5):351-357. https://doi.org/10.1177/2050640613501507

2. Ward SC, Waxman S. Fibrolamellar carcinoma: a review with a focus on genetics and comparison to other malignant primary liver tumors. *Semin Liver Dis*. 2011;31(1):61-70. https://doi.org/10.1055/s-0031-1272835

3. Graham RP, Jin L, Knutson DL, et al. DNAJB1-PRKACA is specific for fibrolamellar carcinoma. *Mod Pathol*. 2015;28(6):822-829. https://doi.org/10.1038/modpathol.2015.4

4. Honeyman JN, Simon EP, Robine N, et al. Detection of a recurrent DNAJB1-PRKACA chimeric transcript in fibrolamellar hepatocellular carcinoma. *Science*. 2014;343(6174):1010-1014. https://doi.org/10.1126/science.1249484

5. Cheung J, Ginter C, Cassidy M, et al. Structural insights into misregulation of protein kinase A in human tumors. *Proc Natl Acad Sci USA*. 2015;112(5):1374-1379. https://doi.org/10.1073/pnas.1424206112

6. Riehle KJ, Yeh MM, Yu JJ, et al. mTORC1 and FGFR1 signaling in fibrolamellar hepatocellular carcinoma. *Mod Pathol*. 2015;28(1):103-110. https://doi.org/10.1038/modpathol.2014.78

7. Riggle KM, Riehle KJ, Kenerson HL, et al. Enhanced cAMP-stimulated protein kinase A activity in human fibrolamellar hepatocellular carcinoma. *Pediatr Res*. 2016;80(1):110-118. https://doi.org/10.1038/pr.2016.36

8. Sastri M, Barraclough DM, Carmichael PT, Taylor SS. A-kinase-interacting protein localizes protein kinase A in the nucleus. *Proc Natl Acad Sci USA*. 2005;102(2):349-354. https://doi.org/10.1073/pnas.0408608102

9. Wiley JC, Wailes LA, Idzerda RL, McKnight GS. Role of regulatory subunits and protein kinase inhibitor (PKI) in determining nuclear localization and activity of the catalytic subunit of protein kinase A. *J Biol Chem*. 1999;274(10):6381-6387.

10. Chen X, Dai JC, Orellana SA, Greenfield EM. Endogenous protein kinase inhibitor gamma terminates immediate-early gene expression induced by cAMP-dependent protein kinase (PKA) signaling: termination depends on PKA inactivation rather than PKA export from the nucleus. *J Biol Chem*. 2005;280(4):2700-2707. https://doi.org/10.1074/jbc.M412558200

11. Chen X, Hausman BS, Luo G, et al. Protein kinase inhibitor gamma reciprocally regulates osteoblast and adipocyte differentiation by downregulating leukemia inhibitory factor. *Stem Cells*. 2013;31(12):2789-2799. https://doi.org/10.1002/stem.1524

12. Lum H, Hao Z, Gayle D, Kumar P, Patterson CE, Uhler MD. Vascular endothelial cells express isoforms of protein kinase A inhibitor. *Am J Physiol Cell Physiol*. 2002;282(1):C59-C66. https://doi.org/10.1152/ajpcell.00256.2001

13. Zheng L, Yu L, Tu Q, et al. Cloning and mapping of human PKIB and PKIG, and comparison of tissue expression patterns of three members of the protein kinase inhibitor family, including PKIA. *Biochem J*. 2000;349(Pt 2):403-407.

14. Studier FW. Protein production by auto-induction in high density shaking cultures. *Protein Expr Purif*. 2005;41(1):207-234.

15. Dostmann WR, Taylor MS, Nickl CK, Brayden JE, Frank R, Tegge WJ. Highly specific, membrane-permeant peptide blockers of cGMP-dependent protein kinase Ialpha inhibit NO-induced cerebral dilation. *Proc Natl Acad Sci USA*. 2000;97(26):14772-14777. https://doi.org/10.1073/pnas.97.26.14772

16. Dostmann WR, Nickl C, Thiel S, Tsigelny I, Frank R, Tegge WJ. Delineation of selective cyclic GMP-dependent protein kinase Ialpha substrate and inhibitor peptides based on combinatorial peptide libraries on paper. *Pharmacol Ther*. 1999;82(2-3):373-387.

17. Sorenson EC, Khanin R, Bamboat ZM, et al. Genome and transcriptome profiling of fibrolamellar hepatocellular carcinoma demonstrates p53 and IGF2BP1 dysregulation. *PLoS One*. 2017;12(5):e0176562. https://doi.org/10.1371/journal.pone.0176562

18. Dinh TA, Vitucci ECM, Wauthier E, et al. Comprehensive analysis of The Cancer Genome Atlas reveals a unique gene and non-coding RNA signature of fibrolamellar carcinoma. *Sci Rep*. 2017;7:44653-44653. https://doi.org/10.1038/srep44653

19. Oikawa T, Wauthier E, Dinh TA, et al. Model of fibrolamellar hepatocellular carcinomas reveals striking enrichment in cancer stem cells. *Nat Commun*. 2015;6:8070. https://doi.org/10.1038/ncomms9070

20. Lalazar G, Simon SM. Fibrolamellar carcinoma: recent advances and unresolved questions on the molecular mechanisms. *Semin Liver Dis*. 2018;38(1):51-59. https://doi.org/10.1055/s-0037-1621710

21. Carson M, Johnson DH, McDonald H, Brouillette C, Delucas LJ. His-tag impact on the structure. *Acta Crystallogr D Biol Crystallogr*. 2007;63(Pt 3):295-301. https://doi.org/10.1107/s0907444906052024

22. Thielges MC, Chung JK, Axup JY, Fayer MD. Influence of histidine tag attachment on picosecond protein dynamics. *Biochemistry.* 2011;50(25):5799-5805. https://doi.org/10.1021/bi2003923

23. Chant A, Kraemer-Pecore CM, Watkin R, Kneale GG. Attachment of a histidine tag to the minimal zinc finger protein of the Aspergillus nidulans gene regulatory protein AreA causes a conformational change at the DNA-binding site. *Protein Expr Purif.* 2005;39(2):152-159. https://doi.org/10.1016/j.pep.2004.10.017

24. Booth WT, Schlachter CR, Pote S, et al. Impact of an N-terminal polyhistidine tag on protein thermal stability. *ACS Omega.* 2018;3(1):760-768. https://doi.org/10.1021/acsomega.7b01598

25. Li DF, Feng L, Hou YJ, Liu W. The expression, purification and crystallization of a ubiquitin-conjugating enzyme E2 from Agrocybe aegerita underscore the impact of His-tag location on recombinant protein properties. *Acta Crystallogr Sect F Struct Biol Cryst Commun.* 2013;69(Pt 2):153-157. https://doi.org/10.1107/s1744309112051755

26. Schumacher J, Bacic T, Staritzbichler R, et al. Enhanced stability of a chimeric hepatitis B core antigen virus-like-particle (HBcAg-VLP) by a C-terminal linker-hexahistidine-peptide. *J Nanobiotechnol.* 2018;16(1):39. https://doi.org/10.1186/s12951-018-0363-0

27. Deng A, Boxer SG. Structural insight into the photochemistry of split green fluorescent proteins: a unique role for a His-tag. *J Am Chem Soc.* 2018;140(1):375-381. https://doi.org/10.1021/jacs.7b10680